European Journal of Radiology 164 (2023) 110850

Contents lists available at ScienceDirect

European Journal of Radiology

journal homepage: www.elsevier.com/locate/ejrad

Meta-analyses

Imaging human lung perfusion with contrast media: A meta-analysis

Lucy Edwards [a], John C Waterton [a,b], Josephine Naish [a,c], Christopher Short [d,e], Thomas Semple [f,g,h], Geoff JM Parker [a,i,*], Marta Tibiletti [a]

[a] Bioxydyn Limited, St James Tower, 7 Charlotte Street, Manchester, M1 4DZ, UK
[b] Centre for Imaging Sciences, University of Manchester, Manchester, UK
[c] MCMR, Manchester University NHS Foundation Trust, Wythenshawe, Manchester, UK
[d] ECFS CTN - LCI Core Facility, Imperial College London, London, UK
[e] Departments of Imaging, Royal Brompton Hospital, Sydney Street, London SW3 6NP, London, UK
[f] Department of Radiology, The Royal Brompton Hospital, London, UK
[g] National Heart and Lung Institute, Imperial College London, London, UK
[h] Centre for Paediatrics and Child Health, Imperial College London, London, UK
[i] Centre for Medical Image Computing, Department of Medical Physics and Biomedical Engineering, University College London, London, UK

ARTICLE INFO

Keywords:
Lung perfusion
Mean Transit Time
Pulmonary Blood Flow
Pulmonary Blood Volume
Indicator dilution theory

ABSTRACT

Purpose: To pool and summarise published data of pulmonary blood flow (PBF), pulmonary blood volume (PBV) and mean transit time (MTT) of the human lung, obtained with perfusion MRI or CT to provide reliable reference values of healthy lung tissue. In addition, the available data regarding diseased lung was investigated.
Methods: PubMed was systematically searched to identify studies that quantified PBF/PBV/MTT in the human lung by injection of contrast agent, imaged by MRI or CT. Only data analysed by 'indicator dilution theory' were considered numerically. Weighted mean (wM), weighted standard deviation (wSD) and weighted coefficient of variance (wCoV) were obtained for healthy volunteers (HV), weighted according to the size of the datasets. Signal to concentration conversion method, breath holding method and presence of 'pre-bolus' were noted.
Results: PBV was obtained from 313 measurements from 14 publications (wM: 13.97 ml/100 ml, wSD: 4.21 ml/100 ml, wCoV 0.30). MTT was obtained from 188 measurements from 10 publications (wM: 5.91 s, wSD: 1.84 s wCoV 0.31). PBF was obtained from 349 measurements from 14 publications (wM: 246.26 ml/100 ml ml/min, wSD: 93.13 ml/100 ml ml/min, wCoV 0.38). PBV and PBF were higher when the signal was normalised than when it was not. No significant differences were found for PBV and PBF between breathing states or between pre-bolus and no pre-bolus. Data for diseased lung were insufficient for *meta*-analysis.
Conclusion: Reference values for PBF, MTT and PBV were obtained in HV. The literature data are insufficient to draw strong conclusions regarding disease reference values.

1. Introduction

Quantification of pulmonary perfusion is important for diagnosis and monitoring of many lung diseases. Some diseases directly involve the pulmonary vasculature, such as pulmonary embolism or pulmonary hypertension. For other pathologies that reduce ventilation, regional perfusion impairment can be caused by hypoxic vasoconstriction according to the Euler-Liljestrand mechanism [1].

Various imaging techniques have been developed to visualise pulmonary perfusion. The current reference standard is pulmonary scintigraphy, which provides semi-quantitative information on lung perfusion using macroaggregates of albumin labelled with technetium-99 m [2].

Magnetic resonance imaging (MRI) combines acquisition of detailed structural images and functional information without ionizing radiation [3]. One of the applications of MRI in the lung is perfusion imaging,

Abbreviations: AIF, Arterial input function; CA, Contrast agent; CDH, Congenital diaphragmatic hernia; COPD, Chronic obstructive pulmonary disease; CT, Computed tomography; CTEPH, Chronic thromboembolic pulmonary hypertension; DECT, Dual-energy computed tomography; FD, Fourier decomposition; HV, Healthy volunteers; MRI, Magnetic resonance imaging; MTT, Mean transit time; PBF, Pulmonary blood flow; PBV, Pulmonary blood volume; PTT, Pulmonary transit time; SPECT, Single-photon emission computerised tomography.

* Corresponding author at: Centre for Medical Image Computing, 1st Floor 90 High Holborn, London WC1V 6LJ, UK.
E-mail address: geoff.parker@ucl.ac.uk (G. JM Parker).

https://doi.org/10.1016/j.ejrad.2023.110850
Received 9 November 2022; Received in revised form 20 April 2023; Accepted 22 April 2023
Available online 27 April 2023
0720-048X/© 2023 The Author(s). Published by Elsevier B.V. This is an open access article under the CC BY license (http://creativecommons.org/licenses/by/4.0/).

which aims to capture the first pass of the bolus of an injected contrast agent (CA), when most of it is still intravascular [4,5]. This MRI technique was first widely applied to the brain [6], but the basic principles can be transferred to all organs, with the difference that in the brain the R_2*, not R_1 changes are typically investigated. It is particularly important for lung imaging, due to the fundamental role of pulmonary perfusion in effective gas exchange [1] and lung function.

The analysis of perfusion imaging datasets requires a conversion from MR signal to CA concentration, and the measurement of the arterial input function (AIF) [4]. The AIF is defined as the concentration of CA over time in the plasma within the feeding artery, typically the pulmonary arteries for the lungs. The most commonly used analysis method is often referred to as the 'indicator dilution theory' [7,8], the outputs of which are pulmonary blood flow, (PBF, typically reported as ml of blood delivered to 100 ml of tissue in a minute ml/100 ml/min), pulmonary blood volume (PBV, typically reported as ml of blood per 100 ml of tissue ml/100 ml), and mean transit time (MTT, typically reported in seconds). An in-depth technical discussion of this method can be found in Sourbron and Buckley [4], but in brief the 'indicator dilution theory' is based on the application of conservation of indicator (tracer) mass and the definition of a probability distribution of transit times, from which MTT is defined. In practice, PBV is typically calculated as the ratio of the area under the curve of the concentration of CA in the lung and the area under the curve in the AIF [9]. PBF is obtained by numerical deconvolution of the concentration curve in the AIF from the concentration curve in the lung [9] and finally, MTT is typically obtained as the ratio of PBV to PBF.

While this quantification method is most commonly applied to MR images, it can also be applied to suitably acquired dynamic computed tomography (CT) images, using appropriate CA [10]. This methodology, however, suffers the significant drawback of high radiation exposure caused by long scanning time[10].

Scintigraphy and single photon emission computed tomography (SPECT) are alternative methods for assessing perfusion and are in widespread clinical use [11]. However, both methods are generally used as qualitative indicators of perfusion deficits, rather than as sources of quantitative perfusion biomarkers [11]. The advantages of quantifying perfusion using MRI over these methods include the lack of ionising radiation; the relative simplicity of tracer preparation and patient management; MRI's higher spatial resolution; and the possibility to acquire anatomical images in the same session. Moreover, with respect to scintigraphy, pulmonary perfusion MRI is often volumetric providing full coverage of both lungs.

The purpose of this *meta*-analysis was to pool and summarise published data of PBF, PBV and MTT in the human lung, obtained with perfusion MRI and CT, and to provide a reliable reference for such biomarkers of healthy lung tissue. Such reference values may be helpful when identifying disease in patients and in testing methods implementation to ensure reasonable results. Potential factors in the imaging acquisitions and in the analysis pipelines that may influence biomarker quantification were also investigated. In addition, the available data regarding these measurements performed in the diseased lung were investigated.

2. Methods

2.1. Literature search

The present study is a *meta*-analysis of published results, and therefore no approval by a local institutional review board was required. A systematic literature search was performed in PubMed on the 26th of November 2021 to identify studies that quantified at least one biomarker among MTT, PBF and PBV in the human lung. A manual search was conducted with the following search terms: *((“Mean Transit Time”[All Fields] OR “Perfusion”[All Fields] OR “DCE”[All Fields] OR (“dynamic”[All Fields] AND (“contrast media”[Pharmacological Action] OR “contrast media”[MeSH Terms] OR (“contrast”[All Fields] AND “media”[All Fields]) OR “contrast media”[All Fields] OR “contrast”[All Fields]) AND (“enhance”[All Fields] OR “enhanced”[All Fields]))AND ((“lung”[MeSH Terms] OR “lung”[All Fields]))) AND (“lung”[MeSH Terms] OR “lung”[All Fields] OR “pulmonary”[All Fields])) AND (“CT”[All Fields] OR “MR”[All Fields] OR “MRI”[All Fields] OR “Computerised Tomography” [All Fields] OR “Magnetic Resonance” [All Fields])*. There were no limits on publication date.

Titles and abstracts of the 2377 results identified in the search were screened by one author. Full-text articles were obtained for the remaining studies requiring a more detailed review. Studies that met any of the following criteria were excluded from the analysis:

- Studies without a quantitative MTT and/or PBF and/or PBV value reported either as mean and standard deviation, median and interquartile changes, or value per individual;
- Values reported only for tumour or other lesions, without lung parenchyma;
- Imaging other than MRI or CT;
- No injection of intravenous contrast agent;
- Studies of phantom / in vitro / animal models without human subjects;
- Reviews and other publication without original data;
- Any language other than English;

2.2. Data analysis

Several data were extracted from each paper. This included the number of subjects and, where available, the mean age. If only the age range was reported, the mean age was estimated to be the arithmetic mean of minimum and maximum age. Data were classified as either 'healthy volunteers' (HV) or 'disease' subjects. Participants that acted as controls had no known underlying lung disease (while possibly having other pathologies) were also classified as HV.

Other extracted data were imaging modality (CT, MRI) and the following imaging parameters: type of CA, dynamic imaging series length, temporal resolution, presence of a pre-bolus injection, and field strength for MRI acquisition. If a range was given instead of a single value for numerical parameters, the arithmetic mean of minimum and maximum values was considered. CA dose information was also noted, and the injected dose was normalised by clinical dose. Since the clinical dose of CA is determined by body weight, normalisation was only possible when the volume injected was expressed as mmol/kg or ml/kg, and not as a fixed volume for all subjects. The described breathing manoeuvres during imaging were noted and classified as expiratory breath-hold, inspiratory breath-hold, free breathing, or no clear volume described. The method used to convert signal to concentration was extracted for MR papers and classified as 'S' (when only a linear relationship between signal and concentration is mentioned), 'S-S0' (when the mean/median of the baseline pre bolus signal S0 is subtracted from the signal S), '(S-S0)/S0' (when the mean/median of the baseline pre bolus signal S0 is subtracted from the signal S and then divided by S0), 'no info' (when no clear information is given).

Mean and standard deviations of MTT, PBF and PBV were also extracted. If the median med, 1st, and 3rd quartiles (q_1, q_3) were all provided in place of the mean, the mean value M and standard deviation SD were estimated as described by Wan et al. [12] as:

$$M = (q_1 + \text{med} + q_3)/3,\ SD = (q_3 - q_1)/1.35$$

If individual data were reported, but no mean/median, mean and SD were then calculated.

The data analysis methods were analysed, including referenced papers if the methodology contained within the manuscript was not considered to be sufficiently clear. For MTT and PBF, only studies where the methods mentioned the application of the 'indicator dilution theory/

theorem' or the execution of a deconvolution were further considered. For PBV, studies that used a 'ratio' of the area under the curve of the signal/concentration of the AIF and lung were also accepted, as this is equivalent to the standard derivation of PBV [4].

The weighted mean and weighted SD (wM, wSD) were calculated for the considered biomarkers from HV studies, weighted by the number of subjects reported in each paper. The weighted coefficient of variation (wCoV) was also calculated as wCoV = wSD/wM. Weighted means were calculated from whole lung measurements and regional measurements. If more than one method was used for the same group of subjects (e.g., a different CA or dose was used), each whole lung measurement output was counted as a separate study, except for measurements designed to assess repeatability. Where multiple regional lung values were reported, their mean was taken to obtain one lung value, to avoid counting one experiment several times, which would introduce a bias towards papers with more complex segmentation. If multiple 'whole lung' regions were reported for the same experiment (e.g., different segmentation methods were implemented as in Risse et al [13]), then only the one chosen as best by the authors was reported. In the case of disease groups, all measurements reported in each study were included to avoid the risk that excessive averaging may dilute the disease effect, given that a pathological process may affect perfusion only in a localised manner. Results with subjects breathing anything other than air were excluded.

2.3. Statistics

Possible linear correlations of MTT, PBV and PBF in HV with the mean age, image resolution and dynamic image series length, were analysed using the Pearson product-moment correlation coefficient [14]. Correlation among the selected biomarkers was also studied in the HV and disease groups in the same fashion. Differences in biomarkers among HV results due to several types of CA injected and breathing manoeuvre executed, were analysed with either parametric tests (a one-way ANOVA or *t*-test) or non-parametric tests (Kruskal-Wallis or Mann-Whitney U ranks test) depending on the results of a Shapiro–Wilk test for normality. Only groups with at least 5 values were included, to avoid problems with homoscedasticity. Pairwise comparison was carried out if one-way ANOVA or Kruskal-Wallis obtained a p-value < 0.05 using a Tukey or a Dunn's test with Bonferroni correction. A p-value$<$0.05 (2-tailed) was considered significant.

3. Results

3.1. Data extraction

The search for keywords returned 2377 records, of these 135 passed a first inspection of title and abstract. Of the remaining 135 records, data were extracted from 46 papers. Of these, 40 were based on MRI and 6

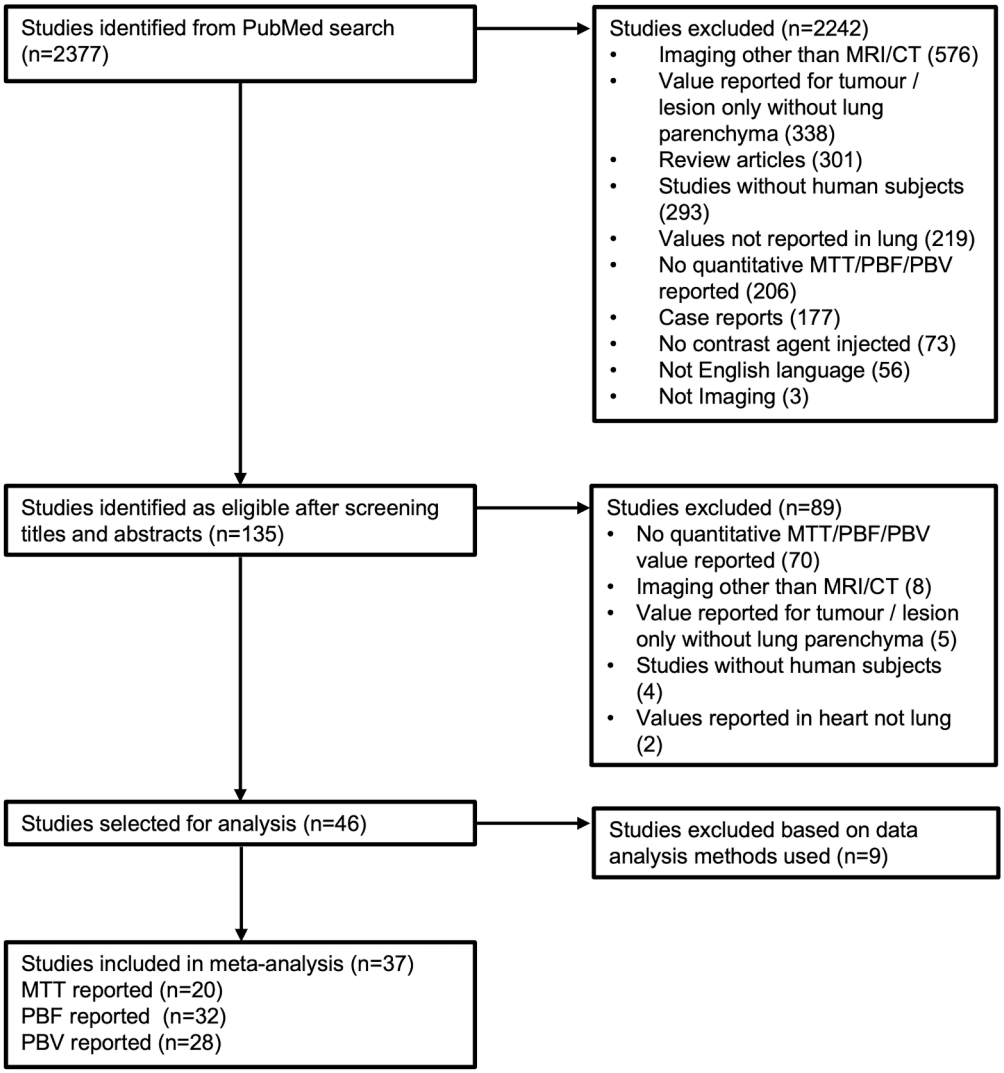

Fig. 1. Flow diagram of the data selection process.

were based on CT. After data extraction, 9 papers were excluded based on the data analysis methods reported, leaving 37 papers available for *meta*-analysis. Fig. 1 presents a flow diagram detailing the data selection process.

PBV was reported in 33 papers in HV and/or diseased subjects. Of these, 29 applied the 'indicator dilution theory' or the ratio of the signal/concentration integrals of the AIF over the tissue to determine PBV. The remaining 4 papers used either a 'One compartment model' (3) or 'Patlak' plot (1); these were excluded to improve the consistency of the results, given the difficulties of comparing analysis methods based on so few cases.

MTT was reported in 30 papers in HV and/or diseased subjects. 20 reported that they applied the 'indicator dilution theory' for data analysis. The remaining papers used the first moment of the tissue signal distribution, either directly (4) or by prior fitting to a gamma variate (3); a 'one compartment model' (1); or the area under the residue curve divided by the maximum height. Finally, one publication reported data without sufficient explanations regarding data extraction [15].

Of the 41 papers reporting PBF values from HV and/or diseased subjects, 32 reported that they analysed data based on the 'indicator dilution theory'. The remaining papers calculated MTT values from the first moment of the tissue signal distribution (4); a 'one compartment model' (3); or by applying semi-quantitative methods (2).

3.2. Healthy volunteer results

Data from HV were available from 17 papers and are described in Table 1. Of the 17 studies, 1 was based on CT and 16 on MRI. All but one performed MRI at 1.5 T field strength. It was therefore not possible to identify if there were systematic differences between imaging modalities and field strength among HV.

Fig. 2 presents all HV data with resulting wM, wSD and 95 % confidence interval. The extracted statistics for PBV are wM: 13.97 ml/100 ml, wSD: 4.21 ml/100 ml, wCoV 0.30, obtained from 313 measurements in 14 publications. The extracted statistics for MTT are wM: 5.91 s, wSD: 1.84 s wCoV 0.31, obtained from 188 measurements in 10 publications. The extracted statistics for PBF are wM: 246.26 ml/100 ml/min, wSD: 93.13 ml/100 ml/min, wCoV 0.38, obtained from 349 measurements in 14 publications.

Regarding the MR acquisitions employed, most had a 3D geometry, and no difference between results in 2D and 3D geometry was found in any biomarker (PBF results: 24 3D, 13 2D, Mann-Whitney U $p = 0.87$; PBV results: 20 3D, 12 2D Mann-Whitney U $p = 0.15$; MTT results, 18 3D, 1 2D, no comparison given small sample size). The most common MR acquisition method was based on a 2D or 3D dynamic GRE acquisition with no preparation, except for Hatabu et al [16] who employed a 2D inversion recovery GRE, Ley et al [17] who employed a 2D saturation recovery GRE, and Oechsner et al [18] and Cao et al [19] who employed

Table 1
Summary of healthy volunteer data from included studies.

Publication	Subjects		Imaging modality	Field strength	Contrast agent	Contrast agent dose	Dynamic series length (s)	Imaging resolution (s)	Breathing manoeuvre/ breath-hold	Biomarker evaluated
	N	Mean age (y)								
Bell et al. 2015 [61]	10	37	MRI	1.5 T	gadopentetate/ gadobenate	0.025 / 0.035 mmol/kg	22	1	expiratory breath-hold	PBF
Cao et al. 2011 [19]	8	48	MRI	1.5 T	gadopentetate	0.01 – 0.07 mmol/kg	n.a	n.a	inspiratory/ expiratory breath-hold	PBF
Fink et al. 2005 [47]	9	28	MRI	1.5 T	gadobenate	0.01 mmol/kg	30	1.5	inspiratory/ expiratory breath-hold	MTT, PBF, PBV
Groß et al. 2021 [30]	10	11.4	MRI	3 T	gadoterate	0.05 mmol/kg	n.a	1.5	free breathing	MTT, PBF, PBV
Hatabu et al. 1999 [62]	6	24.5	MRI	1.5 T	gadopentetate	5 ml	20.16	0.448	breath-hold	PBV
Kuziemski et al. 2011 [10]	8	47.9	CT	n.a	non-ionic contrast medium	40 ml	40	1	inspiratory breath-hold	MTT
Ley et al. 2007 [63]	10	26	MRI	1.5 T	gadopentetate	8 ml	31	0.62	expiratory breath-hold	MTT, PBF, PBV
Ley et al. 2007 [17]	5	41	MRI	1.5 T	gadopentetate	0.1 mmol/kg	37.5	1.5	inspiratory breath-hold	MTT, PBF, PBV
Ley-Zaporozahn et al. 2011 [64]	14	24	MRI	1.5 T	gadopentetate	0.05 mmol/kg	32.5	1.3	inspiratory/ expiratory breath-hold	MTT, PBF, PBV
Oechsner et al. 2009 [18]	11	25	MRI	1.5 T	gadopentetate	0.5 – 3 ml	54	0.3	expiratory breath-hold	PBF, PBV
Ohno et al. 2004 [52]	15	42	MRI	1.5 T	gadopentetate	5 ml	38.5	1.1	inspiratory breath-hold	MTT, PBF, PBV
Ohno et al. 2007 [29]	14	34	MRI	1.5 T	gadopentetate	2 ml	22	1.1	inspiratory breath-hold	MTT, PBF, PBV
Qing et al. 2019 [21]	4	58.8	MRI	1.5 T	gadopentetate	0.2 ml/kg	60	1.8	free breathing	MTT, PBF, PBV
Risse et al. 2006 [65]	5	29	MRI	1.5 T	gadodiamide	0.04–0.09 mmol/kg	40	0.4	inspiratory breath-hold	PBF, PBV
Risse et al. 2009 [13]	7	26	MRI	1.5 T	gadopentetate	0.05 mmol/kg	30	1.5	inspiratory breath-hold	PBF, PBV
Tomasian et al. 2009 [41]	30	28.9	MRI	1.5 T	gadodiamide	0.1 mmol/kg	23	1.2	inspiratory breath-hold	PBV
Veldhoen et al. 2016 [66]	10	23.5	MRI	1.5 T	gadopentetate/ gadofosveset /gadobenate	2.3 – 6.8 / 4.5 – 13.5 / 4.5 – 13.5 ml	26	1.5	expiratory breath-hold	MTT, PBF, PBV

Abbreviations: n.a: not available, N: number, MRI: magnetic resonance imaging, CT: computed tomography, MTT: mean transit time, PBF: pulmonary blood flow, PBV: pulmonary blood volume.

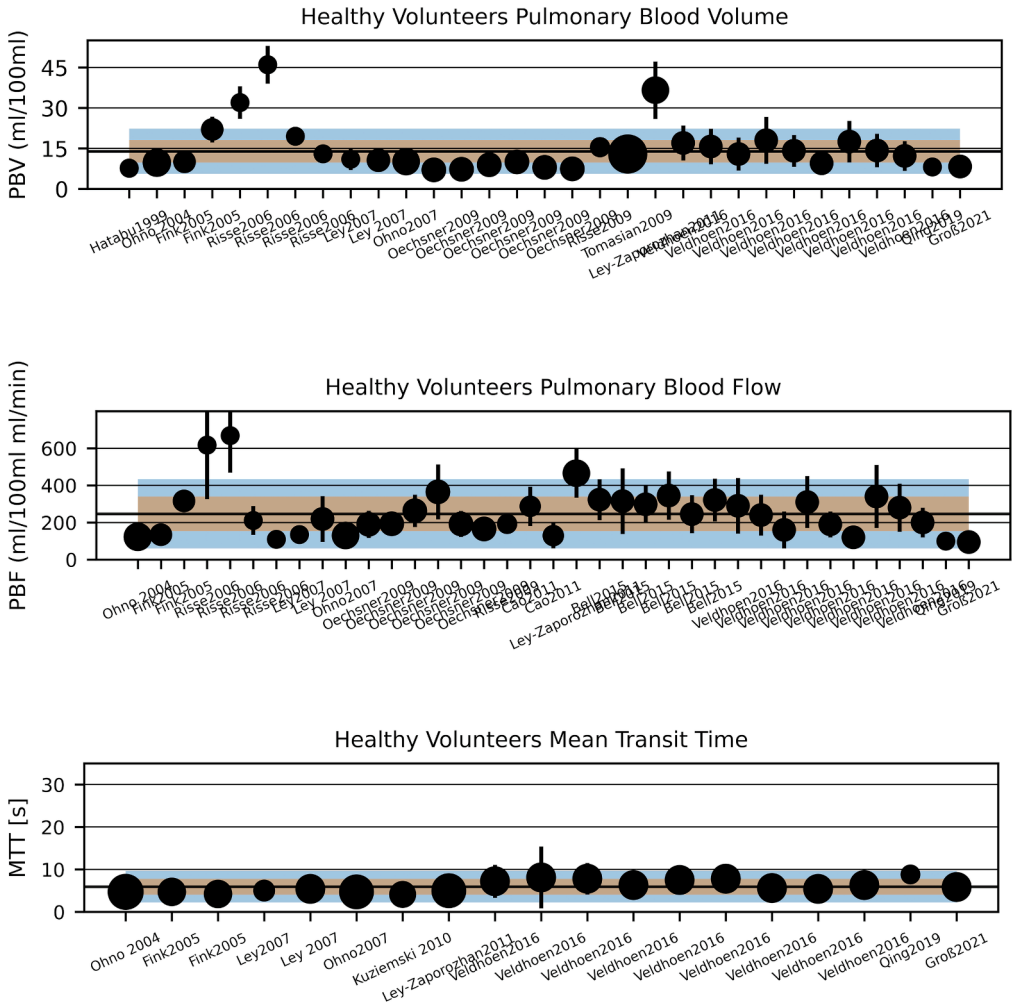

Fig. 2. Mean pulmonary blood volume (PBV) (ml/100 ml), pulmonary blood flow (PBF) (ml/100 ml ml/min) and mean transit time (MTT) (s) in the lung in HV from *meta*-analysis. Each symbol represents whole lung values taken from the listed papers. Symbol size represents group size; symbol error bar represents intra-study SD; horizontal black line is the weighted mean for HV across all studies; shading represents ± 1 and ± 2 wSD of the HV weighted mean.

saturation recovery steady-state free precession.

Regarding the imaging biomarkers considered, the only significant correlation found was that MTT correlated positively with temporal resolution ($p = 0.02$, $R^2 = 0.28$). None of the biomarkers extracted in HV showed a significant correlation with mean age or image acquisition length.

No significant differences were found in any biomarker due to type of CA injected. Among the PBV results, 17 were obtained using gadopentetate, 5 using gadobenate, 4 using gadodiamide, 3 using gadofosveset and 1 with gadoteric acid (Mann-Whitney *U* test gadopentetate acid vs gadobenate acid, $p = 0.07$). Regarding the contrast agent dose considered, a fixed amount of contrast agent was administered for 19 of these results, and a dose proportional to body weight in the remaining 12. For the latter cases, it was possible to extract the ratio of injected dose to clinical dose, which is always given in mmol to body weight, the mean value of which was 0.94 ± 0.48 (range 0.5 to 2.0). No correlation with the proportion of contrast agent to clinical dose and PBV was found (Pearson correlation, $p = 0.51$).

Among the PBF results, 21 were obtained using gadopentetate acid, 8 using gadobenate acid, 4 using gadodiamide, 3 using gadofosveset and 1 with gadoterate (Mann-Whitney U gadopentate vs gadobenate, $p = 0.13$). Regarding the contrast agent dose considered, a fixed amount of contrast agent was administered for 18 of these results, and a dose proportional to body weight in the remaining 19. The mean ratio of injected dose to clinical dose was 0.72 ± 0.5 (range 0.1 to 2.0). No correlation with the proportion of contrast agent to clinical dose and PBV was found (Pearson correlation, $p = 0.53$).

Among the MTT results, 9 were obtained using gadopentetate, 5 using gadobenate, 4 using gadodiamide, 1 with gadoterate and 1 with a non-ionic CT contrast medium (*t*-test, gadopentetate vs gadobenate, $p = 0.21$). Regarding the contrast agent dose considered, a fixed amount of contrast agent was administered for 13 of these results, and a dose proportional to body weight in the remaining 6. The mean ratio of injected dose to clinical dose was 1.17 ± 0.6 (range 0.5 to 2.0). No correlation with the proportion of contrast agent to clinical dose and MTT was found (Pearson correlation, $p = 0.47$).

The most common image acquisition lung volume reported in all studies was 'expiratory breath-hold'. Boxplots comparing inspiration and expiration groups for all biomarkers are shown in Fig. 3A. Of the MTT results, 12 were obtained during expiration, 5 during inspiration, 1 during free breathing and, 1 with no breathing instruction. MTT was significantly higher during expiration than during inspiration (expiration: 6.38 ± 1.23 s, Inspiration: 4.64 ± 0.29 s, *t*-test $p = 0.01$). Among PBF results, 26 were obtained during expiration, 9 during inspiration, 1 during free breathing and, 1 with no breathing instruction. PBF was not significantly different between breathing states (expiration: 260.05 ± 80.22 ml/100 ml ml/min, Inspiration: 257.69 ± 208.52 ml/100 ml ml/min, Mann-Whitney U $p = 0.11$). This is possibly due to two apparent outliers in the inspiratory group, which increase the group SD. Similarly, PBV was not significantly different between lung volumes (expiration:

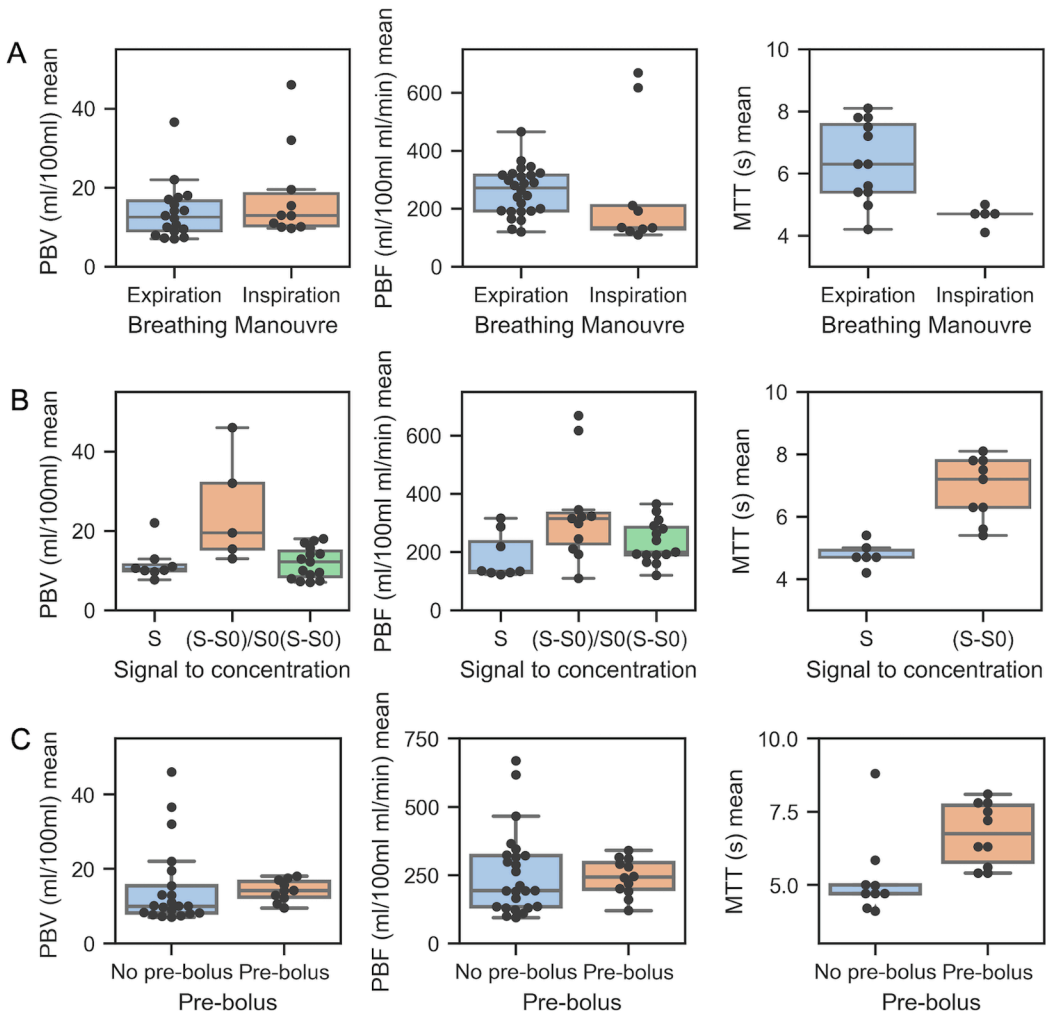

Fig. 3. A) Boxplots representing pulmonary blood volume (PBV), pulmonary blood flow (PBF), and mean transit time (MTT) in healthy volunteers in datasets acquired in 'expiration' and 'inspiration'; B) Boxplots representing PBV, PBF and MTT in healthy volunteers in datasets grouped by MR signal to concentration method. 'S': only a linear relationship between signal and concentration is mentioned; 'S-S0': the mean/median of the baseline pre bolus signal S0 is subtracted from the signal S; '(S-S0)/S0'; the mean/median of the baseline pre bolus signal S0 is subtracted from the signal S and then divided by S0; C) Boxplots representing PBV, PBF and MTT in healthy volunteers in datasets grouped by the presence or lack of a pre-bolus injection ('pre-bolus' vs 'no pre-bolus').

13.82 ± 6.93 ml/100 ml, Inspiration: 17.97 ± 10.80 ml/100 ml, Mann-Whitney U p = 0.33).

Fig. 3B presents a summary of the biomarker results grouped by signal to concentration conversion method. Of the MTT results obtained by MRI, 9 utilised 'S-S0', 6 'S', 3 reported no information. MTT was significantly higher if 'S-S0' was used (6.88 ± 0.95 s) than if 'S' was used (4.78 ± 0.362 s, *t*-test p-value = 0.0003). Among PBF results, 15 were obtained by 'S-S0', 8 by 'S', 11 by '(S-S0)/S0' and 3 reported no information. Multiple comparisons determined that '(S-S0)/S0' obtained higher PBF than 'S' method ('(S-S0)/S0': 331.37 ± 161.68 ml/100 ml ml/min, 'S': 184.01 ± 74.09 ml/100 ml ml/min, p = 0.034). Among PBV results, 15 were obtained by 'S-S0', 8 by 'S', 5 by '(S-S0)/S0′ and 3 reported no information. Multiple comparisons determined that '(S-S0)/S0' obtained higher PBV than 'S - S0' method ('(S-S0)/S0': 25.18 ± 12.29 ml/100 ml, 'S - S0': 11.97 ± 3.82 ml/100 ml, p = 0.034).

Fig. 3C presents the results of papers using a pre-bolus and papers employing a single injection of contrast agent. MTT results were nearly evenly split between the two groups (10 'pre-bolus', 9 'no pre-bolus'). MTT was significantly higher when a pre-bolus was employed ('pre-bolus': 6.74 ± 1.01 s 'no pre-bolus': 5.22 ± 1.35 s, *t*-test p-value = 0.017). It should be noted that significant overlap with the signal to concentration analysis was present since all but one 'pre-bolus' scans where classed as 'S-S0' and most 'no pre-bolus' scans were classed 'S' or 'no info'. No significant differences were found in PBV and PBF in between pre-bolus and no pre-bolus papers (PBF: Mann-Whitney U p-value = 0.74, PBV: Mann-Whitney U p-value = 0.14).

3.3. Disease results

Data from diseased groups were available from 27 papers, which are described in Table 2. Fig. 4 presents all results from diseased groups with HV wM, wSD and 95 % confidence interval for reference.

Among the papers presenting a disease group, 7 studied COPD [20–25], 5 studied pulmonary hypertension [17,26–29], 5 congenital diaphragmatic hernia (CDH) [30–34], 5 chronic thromboembolic pulmonary hypertension (CTEPH) [26,35–38], 1 eisenmenger syndrome (19), 1 pulmonary embolism [26], 1 deep vein thrombosis [39], 1 cystic fibrosis [40], 1 diabetes mellitus [10], 1 tetralogy of fallot [41,26], 1 'pulmonary perfusion deficits' [42], 1 bronchioalveolar carcinoma [43], 2 studies presented groups with mixed diseases [20,36].

Fig. 5 presents the correlation among biomarkers, both in the HV and in the disease population. PBV and PBF showed a strong correlation between each other, in both the healthy and disease groups (HV: $p < 0.001$, $R^2 = 0.76$, Disease $p < 0.001$, $R^2 = 0.79$). This scatterplot also shows a general decrease in PBV and PBF in the disease lungs with respect to HV. A weak negative correlation is present between MTT and PBF in the disease lungs ($R^2 = 0.15$, p-value = 0.0002) but not in the HV ($R^2 = 0.05$, p = 0.36). No correlation is present between PBV vs MTT (HV: $R^2 = 0.05$p = 0.36, Disease: $R^2 = 0.015$, p-value = 0.27).

4. Discussion

In this *meta*-analysis we pooled and summarised values of human lung blood volume, blood flow and mean transit time in the currently

Table 2
Summary of disease group data from included studies.

Publication	Subjects			Modality	Field strength	Contrast agent	Contrast agent dose	Dynamic series length (s)	Imaging resolution (s)	Breathing manoeuvre/ breath-hold	Biomarker evaluated
	N	Mean age (y)	Disease								
Alsady et al. 2021 [35]	19	56.1	CTEPH	MRI	1.5 T	gadoterate	0.04 mmol/kg	n.a	0.8–1.1	Inspiratory breath-hold	PBF, PBV
Fink et al. 2004 [26]	4	44	PE								
	2	44.5	PH	MRI	1.5 T	gadobenate	0.1 mmol/kg	30	1.5	breath-hold	MTT, PBF, PBV
	1	46	CTEPH								
	1	42	Eisenmenger syndrome								
Glandorf et al. 2021 [36]	20	66	COPD	MRI	1.5 T	gadolinium based	0.036 mmol/kg	n.a	n.a	inspiratory breath-hold	PBF
	18	62	CTEPH								
Groß et al. 2021 [30]	54	10.2	CDH	MRI	3 T	gadoterate	0.05 mmol/kg	n.a	1.5	free breathing	MTT, PBF, PBV
Hansch et al. 2012 [39]	31	56	DVT	MRI	1.5 T	gadofosveset	0.03 mmol/kg	332.8	3.2	Inspiratory breath-hold	MTT, PBF, PBV
Hansmann et al. 2013 [42]	18	61	pulmonary perfusion deficits	MRI	3 T	gadoterate	0.07 mmol/kg	58	n.a	Inspiratory breath-hold	MTT, PBF, PBV
Hueper et al. 2013 [44]	123	67.7	COPD & HV	MRI	1.5 T	gadopentetate	0.1 mmol/kg	60	1.5	inspiratory breath-hold	PBV
Jang et al. 2008 [20]	14	68.1	COPD	MRI	1.5 T	gadopentetate	0.2 mmol/ml	35	1	Inspiratory breath-hold	PBV
Kaireit et al. 2017 [40]	16	14.5	CF	MRI	1.5 T	gadoterate	0.03 mmol/kg	32–40	0.9	Inspiratory breath-hold	PBF
Kaireit et al. 2019 [25]	47	61	COPD	MRI	1.5 T	gadobutrol	0.025 mmol/kg	n.a	n.a	Inspiratory breath-hold	PBF
Kuziemski et al. 2011 [10]	10	45.3	Diabetes mellitus	CT	n.a	non-ionic contrast medium	40 ml	40	1	inspiratory breath-hold	MTT
Ley et al. 2007 [17]	20	41	PH	MRI	1.5 T	gadopentetate	0.1 mmol/kg	37.5	1.5	free breathing	MTT, PBF, PBV
Ley et al. 2013 [27]	20	54/47	PH	MRI	1.5 T	gadopentetate	0.1 mmol/kg	37.5	1.5	inspiratory breath-hold	MTT, PBF, PBV
Ohno et al. 2004 [52]	25	61	PH & COPD, PH & CTEPH, PH	MRI	1.5 T	gadopentetate	5 ml	38.5	1	inspiratory breath-hold	MTT, PBF, PBV
Ohno et al. 2006 [36]	40	72	BAC	MRI	1.5 T	gadopentetate	0.1–0.5 mmol/ml	26	1.3	expiratory breath-hold	MTT, PBF, PBV
Ohno et al. 2007 [29]	14	41	PH	MRI	1.5 T	gadopentetate	2 ml	20	1	expiratory breath-hold	MTT, PBF, PBV
Qing et al. 2019 [21]	4	61	COPD	MRI	1.5 T	gadopentetate	0.2 mmol/kg	60	1.8	free breathing	MTT, PBF, PBV
Schiwek et al. 2021 [22]	83	65.7	COPD	MRI	1.5 T	gadobutrol	2 ml	33	1.6	inspiratory breath-hold	PBV
Schoenfeld et al. 2016 [37]	19	50	CTEPH	MRI	1.5 T	gadoterate	0.04 mmol/kg	40–48	1–1.2	inspiratory breath-hold	PBF
Schoenfeld et al. 2019 [38]	29	72	CTEPH	MRI	1.5 T	gadoterate	0.04 mmol/kg	40–48	1–1.2	inspiratory breath-hold	PBF
Sergiacomi et al. 2014 [23]	15	71.4	COPD	MRI	3 T	gadopentetate	0.5 mmol/ml	15	1.5	inspiratory breath-hold	PBV
Ter-Karapetyan et al. 2018 [24]	19	66	COPD	MRI	1.5 T	gadopentetate	0.05 mmol/kg	37	1.47	inspiratory breath-hold	MTT, PBF, PBV
Tomasian et al. 2009 [41]	30	29.6	TOF	MRI	1.5 T	gadodiamide	0.1 mmol/kg	23	1.2	Inspiratory breath-hold	PBV
Weidner et al. 2014 [31]	18	2	CDH	MRI	3 T	gadoterate	0.05 mmol/kg	144	1.5/3	free breathing	MTT, PBF, PBV
Weis et al. 2016 [32]	38	2	CDH	MRI	3 T	gadoterate	0.05 mmol/kg	84	1.5	free breathing	MTT, PBF, PBV
Weis et al. 2016 [32]	30	2	CDH	MRI	3 T	gadoterate	0.05 mmol/kg	75	1.5	free breathing	MTT, PBF, PBV
Zöllner et al. 2012 [34]	12	2	CDH	MRI	3 T	gadoterate	0.05 mmol/kg	83	3	free breathing	MTT, PBF, PBV

Abbreviations: n.a: not available, MRI: magnetic resonance imaging, CT: computed tomography, PE: pulmonary embolism, PH: pulmonary hypertension, CTEPH: chronic thromboembolic pulmonary hypertension, COPD: chronic obstructive pulmonary disease, CDH: congenital diaphragmatic hernia, DVT: deep vein thrombosis, CF: cystic fibrosis, BAC: bronchioalveolar carcinoma, TOF: tetralogy of Fallot, MTT: mean transit time, PBF: pulmonary blood flow, PBV: pulmonary blood volume.

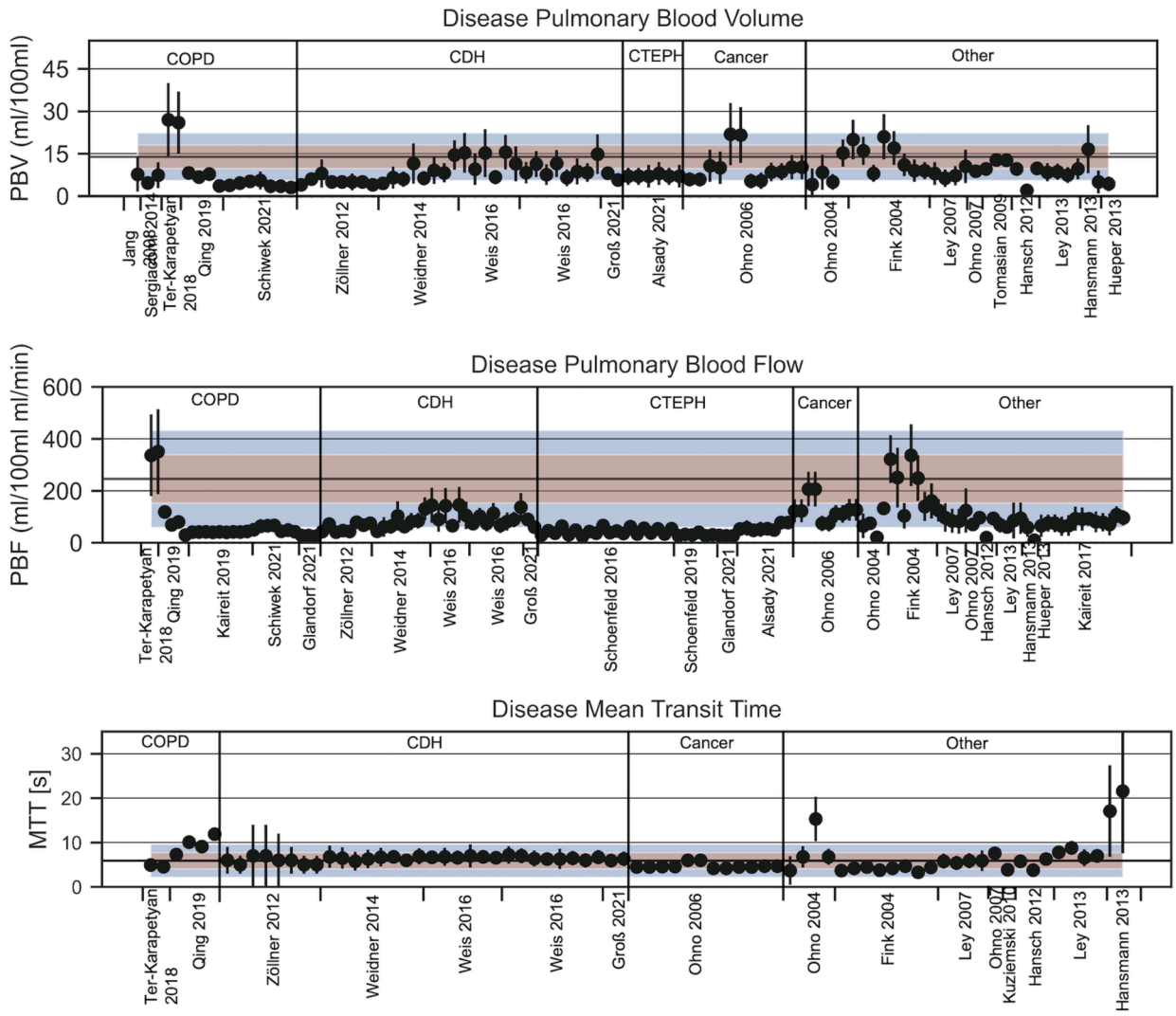

Fig. 4. Mean pulmonary blood volume (PBV) (ml/100 ml), pulmonary blood flow (PBF) (ml/100 ml ml/min) and mean transit time (MTT) (s) in the lung in disease groups. Symbol size represents group size; symbol error bar represents intra-study SD; horizontal black line is the weighted mean for HV across all studies; shading represents ± 1 and ± 2 SD of the HV weighted mean. All values reported in each paper are shown.

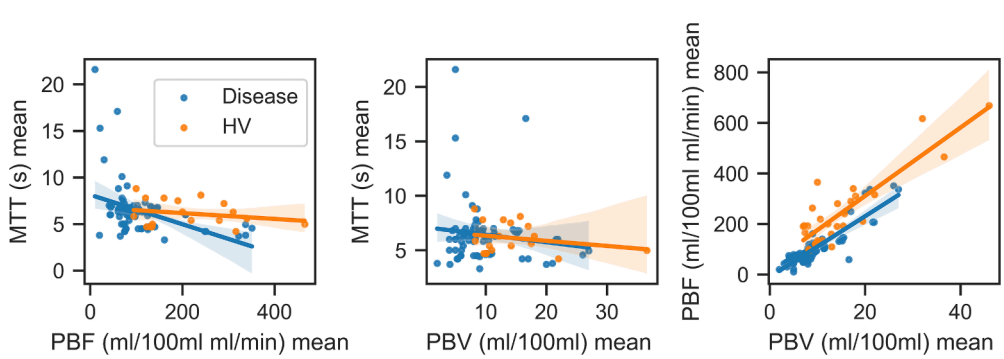

Fig. 5. Scatterplots representing the correlations between pulmonary blood flow (PBF), pulmonary blood volume (PBV) and mean transit time (MTT) in the healthy volunteers' group (orange symbols) and disease group (blue symbols). The straight line represents the best linear fit for each group and the shaded area is the 95 % confidence area.

available literature. Our results provide normative data of PBF, PBV and MTT in adult subjects, which may be compared to results obtained in patients with specific lung pathologies.

We chose to numerically evaluate only results obtained by the 'indicator dilution theory' to improve comparability of methods and due to the likely more meaningful results that this method can provide. Specifically, Weisskoff [8] explained extensively why the first moment of the concentration time curve is not equivalent to the ratio of PBV to PBF in the realistic blood circulation system, and it is therefore not a comparable method to calculate MTT. We have also verified in this work that the 'indicator dilution theory' was indeed by far the prevailing analysis method in the literature.

PBF was the most quantified parameter, with 32 papers presenting results from healthy volunteers; PBV was calculated in 28 publications, and MTT in only 20. The coefficients of variation for all three biomarkers were similar (range 0.30 for PBV, 0.31 for MTT to 0.38 for PBF).

Regarding the method used to convert MR signal to concentration of CA, no paper used a calculated T_1 map, which is typical in dynamic contrast-enhanced studies in other parts of the body [45], as it is the mathematically corrected method. A linear correlation between signal (S), signal minus baseline (S-S0) or signal minus baseline over baseline ((S-S0)/S0) is instead assumed. The latter method resulted in the highest PBF and PBV results. In fact, PBF and PBV results obtained by S and (S-S0) results are weighted by lung density, given the intrinsic weighting by spin density present in the MR signal. In contrast, ((S-S0)/S0) and T_1-based methods are not weighted by lung density, given that in the former the presence of the division step cancels the spin density and, in the latter, the T_1 estimation decouples T_1 and spin density effects. MTT does not suffer from this issue since it is calculated as PBF/PBV, therefore cancelling density effects. We note that ((S-S0)/S0) or a T_1-based calculation are only possible if sufficient SNR is achieved at baseline in lung parenchyma, and while this is clearly possible with modern scanners, it may have not been the case in all the acquisitions considered here. More work is needed to investigate the effects of this key part of the analysis pipeline, in healthy subjects and diseases that significantly modify lung density, such as emphysema or fibrosis. It is also notable that a few papers did not clearly report the method used. Given the importance that this step of the analysis has on the result interpretation, we would like to recommend to all authors to clearly specify how the signal is dealt with.

The issue of non-linearity at high CA concentration is sometimes dealt with in a separate 'pre-bolus' scan whose AIF is then rescaled to be used in the 'bolus' scan, which has higher SNR in the lung. In the case of MTT, it was not possible to discern if the biomarker was influenced by use of the conversion method or the pre-bolus given the significant overlap between 'pre-bolus' and 'S-S0' groups and 'no pre-bolus' and 'S' groups. For PBV and PBF, no significant effect of pre-bolus was found. This is a potentially useful observation, as it suggests that the additional effort and time required to make use of a 'pre-bolus' scan may be of limited value, enabling shorter scanning sessions and lower overall CA dose.

A strong correlation between PBF and PBV was found both in HV and diseased lung. PBV correlated with MTT only in diseased lung, and no correlation was present between PBF and MTT. Since MTT is defined as PBV/PBF, effectively meaning any increase in PBF is generally cancelled out by an increase in PBV.

Our findings do not demonstrate a strong dependence between calculated biomarkers and imaging parameters or type of injected contrast agent, which is a reassuring indicator of biomarker robustness to varying data acquisition and analysis methods.

We also found no biomarker dependency on age; however, most datasets represented HV between 20 and 50 years of age, so we cannot exclude that age dependency could emerge if including older or younger subjects, particularly as children as the lung is still developing well into the late teens [46]. MTT was found to correlate positively with temporal resolution. Most works reporting MTT used a temporal resolution of 1.5 s, with only in one work a higher value (interval 0.6–1.8 s), therefore the significance of this correlation may be questioned. No significant correlation was found between PBV and PBF and temporal resolution.

Comparing results by breathing manoeuvre gave mixed results. A change in PBV might be expected [47], but instead MTT was found to be slightly higher in expiration than in inspiration, in contrast to what was obtained by Fink et al [40]. While this might be explained by the linear dependence of MTT on PBV, this explanation is not supported by the data. One limitation is that a variety of breathing manoeuvres were described in the literature, since dynamic imaging duration is often too long to accommodate a single breath-hold, so each category (i.e., 'inspiration'/'expiration') was not uniform. Also, most authors preferred an 'expiration' breath-hold, therefore the two groups were unbalanced. This preference is present due to the increased available baseline parenchyma MR signal in expiration, despite the greater difficulty in maintaining an expiratory breath-hold relative to an inspiratory breath-hold, particularly in patients with reduced respiratory function.

Another reason to avoid a full inspiratory breath-hold is that this may result in an involuntary Valsalva manoeuvre, where an increase in intrathoracic pressure during breath-hold leads to a decrease in cardiac output and total lung perfusion [48,49]. Clear instructions of respiratory manoeuvres are known to play a significant role in reproducible pulmonary arterial imaging [50] with potential implications for first pass perfusion measurements. While the clinical standard imaging method to estimate lung perfusion is by nuclear medicine, direct comparison of quantitative results obtained with this method and MRI, or CT perfusion imaging cannot be achieved. The reason is that scintigraphy is based on counting radionuclide decay events in the lung, which are delivered by injection of macroaggregates of albumin and depends on the principle that particles of appropriate size are trapped in the lung at first passage in direct proportion to the local rate of blood flow [2], but it does not quantify the local blood flow in volumetric units. Some works have attempted to compare lung perfusion by MR and scintigraphy [47], but these are based on calculating the ratio of PBF between different regions of interest [51], not on direct comparison of quantitative values [42,43].

An alternative approach to obtain perfusion-related information using MR imaging is Fourier decomposition (FD) MRI. FD MRI provides regional perfusion (Q) and ventilation (V) information from a single acquisition series, exploiting the spectral separation of the respiratory and cardiac signal modulations in the pulmonary parenchyma [53]. Kjørstadt et al [54] found values of PBF in 9 HV around 150 ml/100 ml/min, which is at the low end of the range found in this work. Bauman and Bieri [53] estimated PBF in volunteers with FD MRI and obtained results around or above 200 ml/100 ml/min, which are more in line with our findings from the literature.

PBV can also be calculated with Dual Energy CT (DECT), which acquires simultaneous images at high and low-energy x-ray spectra [55]. The basic principle of dual-energy CT is material decomposition based on attenuation differences at different energy levels. The lung is an example of a three-component system, consisting of air, soft tissue, and injected iodine in the blood stream [56]. Given the radiation exposure, 'healthy' subjects are not typically imaged with this technique. Moreover, data are not necessarily reported in a unit (HU) that can be compared easily with our findings [57]. Thus, comparison of DECT derived PBV and MRI derived PBV in healthy subjects is not straightforward. Alsady et al [35] directly compared PBV by MRI and DECT in CTEPH patients, and obtained significantly different results, which they in part attributed to the dependency of the absolute pulmonary iodine concentration on cardiac function.

It also should be noted that there is a corpus of research involving 'pulmonary transit time' (PTT), defined as the time necessary for a contrast bolus to pass from the right- to left-sided circulation [58]. MTT and PTT are similarly named but cannot be directly compared. Kanski et al [59] measured PTT and cardiac output using cardiac MRI and obtained a whole lung PBV by multiplying the two parameters and dividing by lung volume. In HV, a PBV of 20 ± 5 % was found, which is higher

than obtained in this work.

We did not consider the available data on diseased subjects to be of sufficient quality and uniformity to attempt a *meta*-analysis. Even so, visualising available data as in Figs. 4 and 5, clearly pinpoint that PBF and PBV are low in all considered disease. MTT appears largely similar in the considered diseases to that in the healthy lung, reflecting its definition as the ratio of PBV to PBF. It can also be noted that not all lung pathologies have been investigated by the methodology investigated in this work, with fibrotic lung disease being a particularly common disease category missing.

Future work on this topic should concentrate on improving reporting of the analysis method, since this is necessary to improve data reproducibility, as steps like the signal-to-concentration conversion and the method used to deconvolve the impulse function [60] have significant impact on the results. To this end, researchers should be encouraged to share their analysis code.

4.1. Limitations

This paper has some limitations beyond the ones already mentioned. Regarding papers reporting HV results, only one based on CT was available. Regarding the MR publications, all but one made use of 1.5 T. Therefore, it was not possible to identify if there were systematic differences between imaging methods and field strength among HV results. Contrast agent dose information could only be partially studied due to inconstancy: dose by weight and fixed dose were both commonly used and could not be reconciled due to lack of weight information. When dose by weight was present, this was normalised with the recommended clinical dose, and no correlation with perfusion biomarkers was found with normalised dose. Moreover, the insufficient amount of data in the available literature does not allow for studying the interplay between various analysis methods and acquisition parameters, and therefore some effects may be hidden.

5. Conclusion

In conclusion, in this *meta*-analysis we obtained normative values for PBF, PBV and MTT from the currently available literature in perfusion imaging. Given the relative complex analysis involved, future work on this topic should concentrate on improving reporting of the analysis method, to improve data reproducibility.

CRediT authorship contribution statement

Lucy Edwards: Data curation, Formal analysis, Investigation, Methodology, Visualization, Writing – original draft, Writing – review & editing. **John C Waterton:** Conceptualization, Funding acquisition, Supervision, Writing – review & editing. **Jo Naish:** Writing – review & editing. **Christopher Short:** Writing – review & editing. **Thomas Semple:** Writing – review & editing. **Geoff JM Parker:** Funding acquisition, Supervision, Writing – review & editing. **Marta Tibiletti:** Investigation, Methodology, Software, Supervision, Visualization, Writing – original draft, Writing – review & editing.

Declaration of Competing Interest

The authors declare the following financial interests/personal relationships which may be considered as potential competing interests: [Geoffrey Parker reports financial support was provided by Innovative Medicines Initiatives 2. Lucy Edwards reports financial support was provided by Innovative Medicines Initiatives 2. John C Waterton reports financial support was provided by Innovative Medicines Initiatives 2. Marta Tibiletti reports financial support was provided by Innovative Medicines Initiatives 2. Jo Naish reports financial support was provided by Innovative Medicines Initiatives 2. Lucy Edwards reports a relationship with Bioxydyn Ltd that includes: employment. John C Waterton reports a relationship with Quantitative Imaging Ltd that includes: equity or stocks. John C Waterton reports a relationship with Bioxydyn Ltd that includes: board membership and employment. Josephine Naish reports a relationship with Bioxydyn Ltd that includes: employment. Christopher Short reports a relationship with Vertex Pharmaceuticals Incorporated that includes: speaking and lecture fees. Thomas Semple reports a relationship with Vertex Pharmaceuticals Incorporated that includes: speaking and lecture fees. Thomas Semple reports a relationship with Chiesi Pharmaceuticals that includes: funding grants. Thomas Semple reports a relationship with Boehringer Ingelheim Ltd that includes: consulting or advisory. Thomas Semple reports a relationship with Calyx Ltd that includes: consulting or advisory. Geoffrey Parker reports a relationship with Quantitative Imaging Ltd that includes: board membership and equity or stocks. Geoffrey Parker reports a relationship with Queen Square Analytics Ltd that includes: board membership and equity or stocks. Geoffrey Parker reports a relationship with Bioxydyn Ltd that includes: board membership and employment. Marta Tibiletti reports a relationship with Quantitative Imaging Ltd that includes: equity or stocks. Marta Tibiletti reports a relationship with Bioxydyn Ltd that includes: board membership and employment.].

Acknowledgements

The research leading to these results received funding from the Innovative Medicines Initiatives 2 Joint Undertaking under grant agreement No 116106. This Joint Undertaking receives support from the European Union's Horizon 2020 research and innovation programme and EFPIA. The views expressed are those of the authors and not necessarily those of the TRISTAN consortium.

References

[1] N. Sommer, A. Dietrich, R.T. Schermuly, H.A. Ghofrani, T. Gudermann, R. Schulz, W. Seeger, F. Grimminger, N. Weissmann, Regulation of hypoxic pulmonary vasoconstriction: Basic mechanisms, Eur. Respir. J. 32 (2008) 1639–1651, https://doi.org/10.1183/09031936.00013908.

[2] K. Zöphel, C. Bacher-Stier, J. Pinkert, J. Kropp, Ventilation/perfusion lung scintigraphy: what is still needed? A review considering technetium-99m-labeled macro-aggregates of albumin, Ann. Nucl. Med. 23 (2009) 1–16, https://doi.org/10.1007/s12149-008-0187-3.

[3] M. Wielputz, H. Kauczor, MRI of the lung: State of the art, Diagn. Interv. Radiol. 18 (2012) 344–353, https://doi.org/10.4261/1305-3825.DIR.5365-11.0.

[4] S.P. Sourbron, D.L. Buckley, Classic models for dynamic contrast-enhanced MRI, NMR Biomed. 26 (2013) 1004–1027, https://doi.org/10.1002/nbm.2940.

[5] R.I. Pettigrew, L. Avruch, W. Dannels, J. Coumans, M.E. Bernardino, Fast-field-echo MR imaging with Gd-DTPA: physiologic evaluation of the kidney and liver, Radiology 160 (1986) 561–563, https://doi.org/10.1148/radiology.160.2.3726139.

[6] A. Villringer, B.R. Rosen, J.W. Belliveau, J.L. Ackerman, R.B. Lauffer, R.B. Buxton, Y.-S. Chao, V.J. Wedeenand, T.J. Brady, Dynamic imaging with lanthanide chelates in normal brain: Contrast due to magnetic susceptibility effects, Magn. Reson. Med. 6 (1988) 164–174, https://doi.org/10.1002/mrm.1910060205.

[7] K.L. Zierler, Theoretical basis of indicator-dilution methods for measuring flow and volume, Circ. Res. 10 (1962) 393–407, https://doi.org/10.1161/01.RES.10.3.393.

[8] R.M. Weisskoff, D. Chesler, J.L. Boxerman, B.R. Rosen, Pitfalls in MR measurement of tissue blood flow with intravascular tracers: Which mean transit time? Magn. Reson. Med. 29 (1993) 553–558, https://doi.org/10.1002/mrm.1910290420.

[9] S. Sourbron, R. Luypaert, P. Van Schuerbeek, M. Dujardin, T. Stadnik, M. Osteaux, Deconvolution of dynamic contrast-enhanced MRI data by linear inversion: Choice of the regularization parameter, Magn. Reson. Med. 52 (2004) 209–213, https://doi.org/10.1002/mrm.20113.

[10] K. Kuziemski, J. Pieńkowska, W. Słomiński, K. Specjalski, K. Dziadziuszko, E. Jassem, M. Studniarek, R. Kalicka, J.M. Słomiński, Role of quantitative chest perfusion computed tomography in detecting diabetic pulmonary microangiopathy, Diabetes Res. Clin. Pract. 91 (2011) 80–86, https://doi.org/10.1016/j.diabres.2010.11.004.

[11] S.R. Hopkins, M.O. Wielpütz, H.-U. Kauczor, Imaging lung perfusion, J. Appl. Physiol. 113 (2012) 328–339, https://doi.org/10.1152/japplphysiol.00320.2012.

[12] X. Wan, W. Wang, J. Liu, T. Tong, Estimating the sample mean and standard deviation from the sample size, median, range and/or interquartile range, BMC Med. Res. Method. 14 (2014) 135, https://doi.org/10.1186/1471-2288-14-135.

[13] F. Risse, T.A. Kuder, H.U. Kauczor, W. Semmler, C. Fink, Suppression of pulmonary vasculature in lung perfusion MRI using correlation analysis, Eur. Radiol. 19 (2009) 2569–2575, https://doi.org/10.1007/s00330-009-1464-9.

[14] D.R. Freedman, R. Pisani, R. Purves, Statistics, 4th ed., W. W. Norton & Company, New York, 2007.

[15] H. Sun, F. Gao, N. Li, C. Liu, An evaluation of the feasibility of assessment of volume perfusion for the whole lung by 128-slice spiral CT, Acta Radiol. 54 (2013) 921–927, https://doi.org/10.1177/0284185113490151.
[16] H. Hatabu, E. Tadamura, D.L. Levin, Q. Chen, W. Li, D. Kim, P.V. Prasad, R. R. Edelman, Quantitative assessment of pulmonary perfusion with dynamic contrast-enhanced MRI, Magn. Reson. Med. 42 (1999) 1033–1038, https://doi.org/10.1002/(SICI)1522-2594(199912)42:6<1033::AID-MRM7>3.0.CO;2-7.
[17] S. Ley, D. Mereles, F. Risse, E. Grünig, J. Ley-Zaporozhan, Z. Tecer, M. Puderbach, C. Fink, H.U. Kauczor, Quantitative 3D pulmonary MR-perfusion in patients with pulmonary arterial hypertension: Correlation with invasive pressure measurements, Eur. J. Radiol. 61 (2007) 251–255, https://doi.org/10.1016/j.ejrad.2006.08.028.
[18] M. Oechsner, M. Mühlhäusler, C.O. Ritter, M. Weininger, M. Beissert, P.M. Jakob, M. Beer, D. Hahn, H. Köstler, Quantitative contrast-enhanced perfusion measurements of the human lung using the prebolus approach, J. Magn. Reson. Imaging 30 (2009) 104–111, https://doi.org/10.1002/jmri.21793.
[19] J.J. Cao, Y. Wang, W. Schapiro, J. McLaughlin, J. Cheng, M. Passick, N. Ngai, P. Marcus, N. Reichek, Effects of respiratory cycle and body position on quantitative pulmonary perfusion by MRI, J. Magn. Reson. Imaging 34 (2011) 225–230, https://doi.org/10.1002/jmri.22527.
[20] Y.M. Jang, Y.-M. Oh, J.B. Seo, N. Kim, E.J. Chae, Y.K. Lee, S. do Lee, Quantitatively Assessed Dynamic Contrast-Enhanced Magnetic Resonance Imaging in Patients With Chronic Obstructive Pulmonary Disease: Correlation of Perfusion Parameters With Pulmonary Function Test and Quantitative Computed Tomography, Investigative Radiology 43 (2008) 403–410, https://doi.org/10.1097/RLI.0b013e31816901ab.
[21] K. Qing, N.J. Tustison, J.P. Mugler, J.F. Mata, Z. Lin, L. Zhao, D. Wang, X. Feng, J. Y. Shin, S.J. Callahan, M.P. Bergman, K. Ruppert, T.A. Altes, J.M. Cassani, Y. M. Shim, Probing changes in lung physiology in COPD using CT, perfusion MRI, and hyperpolarized xenon-129 MRI, Acad. Radiol. 26 (2019) 326–334, https://doi.org/10.1016/j.acra.2018.05.025.
[22] M. Schiwek, S.M.F. Triphan, J. Biederer, O. Weinheimer, M. Eichinger, C. F. Vogelmeier, R.A. Jörres, H.U. Kauczor, C.P. Heußel, P. Konietzke, O. von Stackelberg, F. Risse, B.J. Jobst, M.O. Wielpütz, Quantification of pulmonary perfusion abnormalities using DCE-MRI in COPD: Comparison with quantitative CT and pulmonary function, Eur. Radiol. 32 (2021) 1879–1890, https://doi.org/10.1007/s00330-021-08229-6.
[23] G. Sergiacomi, A. Taglieri, A. Chiaravalloti, E. Calabria, S. Arduini, D. Tosti, D. Citraro, G. Pezzuto, E. Puxeddu, G. Simonetti, Acute COPD exacerbation: 3 T MRI evaluation of pulmonary regional perfusion - preliminary experience, Respir. Med. 108 (2014) 875–882, https://doi.org/10.1016/j.rmed.2014.04.002.
[24] A. Ter-Karapetyan, S.M.F. Triphan, B.J. Jobst, A.F. Anjorin, J. Ley-Zaporozhan, S. Ley, O. Sedlaczek, J. Biederer, H.U. Kauczor, P.M. Jakob, M.O. Wielpütz, Towards quantitative perfusion MRI of the lung in COPD: The problem of short-term repeatability, PLoS One 13 (2018), e0208587, https://doi.org/10.1371/journal.pone.0208587.
[25] T.F. Kaireit, A. Voskrebenzev, M. Gutberlet, J. Freise, B. Jobst, H.U. Kauczor, T. Welte, F. Wacker, J. Vogel-Claussen, Comparison of quantitative regional perfusion-weighted phase resolved functional lung (PREFUL) MRI with dynamic gadolinium-enhanced regional pulmonary perfusion MRI in COPD patients, J. Magn. Reson. Imaging 49 (2019) 1122–1132, https://doi.org/10.1002/jmri.26342.
[26] C. Fink, F. Risse, R. Buhmann, S. Ley, F.J. Meyer, C. Plathow, M. Puderbach, H. U. Kauczor, Quantitative Analysis of pulmonary perfusion using time-resolved parallel 3D MRI - initial results, RoFo Fortschritte Auf Dem Gebiet Der Rontgenstrahlen Und Der Bildgebenden Verfahren. 176 (2004) 170–174, https://doi.org/10.1055/s-2004-817624.
[27] S. Ley, C. Fink, F. Risse, N. Ehlken, C. Fischer, J. Ley-Zaporozhan, H.U. Kauczor, H. Klose, E. Gruenig, Magnetic resonance imaging to assess the effect of exercise training on pulmonary perfusion and blood flow in patients with pulmonary hypertension, Eur. Radiol. 23 (2013) 324–331, https://doi.org/10.1007/s00330-012-2606-z.
[28] Y. Ohno, H. Hatabu, K. Murase, T. Higashino, H. Kawamitsu, H. Watanabe, D. Takenaka, M. Fujii, K. Sugimura, Quantitative assessment of regional pulmonary perfusion in the entire lung using three-dimensional ultrafast dynamic contrast-enhanced magnetic resonance imaging: Preliminary experience in 40 subjects, J. Magn. Reson. Imaging 20 (2004) 353–365, https://doi.org/10.1002/jmri.20137.
[29] Y. Ohno, H. Hatabu, K. Murase, T. Higashino, M. Nogami, T. Yoshikawa, K. Sugimura, Primary pulmonary hypertension: 3D dynamic perfusion MRI for quantitative analysis of regional pulmonary perfusion, Am. J. Roentgenol. 188 (2007) 48–56, https://doi.org/10.2214/AJR.05.0135.
[30] V. Groß, K. Zahn, K. Maurer, L. Wessel, T. Schaible, S.O. Schoenberg, C. Weiß, F. G. Zoellner, M. Weis, MR lung perfusion measurements in adolescents after congenital diaphragmatic hernia: correlation with spirometric lung function tests, Eur. Radiol. 4 (2022) 2572–2580, https://doi.org/10.1007/s00330-021-08315-9.
[31] M. Weidner, F.G. Zöllner, C. Hagelstein, K. Zahn, T. Schaible, S.O. Schoenberg, L. R. Schad, K.W. Neff, High temporal versus high spatial resolution in MR quantitative pulmonary perfusion imaging of two-year old children after congenital diaphragmatic hernia repair, Eur. Radiol. 24 (2014) 2427–2434, https://doi.org/10.1007/s00330-014-3304-9.
[32] M. Weis, V. Sommer, F.G. Zöllner, C. Hagelstein, K. Zahn, T. Schaible, S. O. Schoenberg, K.W. Neff, Region of interest-based versus whole-lung segmentation-based approach for MR lung perfusion quantification in 2-year-old children after congenital diaphragmatic hernia repair, Eur. Radiol. 26 (2016) 4231–4238, https://doi.org/10.1007/s00330-016-4330-6.
[33] M. Weis, F.G. Zoellner, C. Hagelstein, S.O. Schoenberg, K. Zahn, T. Schaible, K. W. Neff, Lung perfusion MRI after congenital diaphragmatic hernia repair in 2-year-old children with and without extracorporeal membrane oxygenation therapy, Am. J. Roentgenol. 206 (2016) 1315–1320, https://doi.org/10.2214/AJR.15.14860.
[34] F.G. Zöllner, K. Zahn, T. Schaible, S.O. Schoenberg, L.R. Schad, K.W. Neff, Quantitative pulmonary perfusion imaging at 3.0 T of 2-year-old children after congenital diaphragmatic hernia repair: Initial results, Eur. Radiol. 22 (2012) 2743–2749, https://doi.org/10.1007/s00330-012-2528-9.
[35] T.M. Alsady, T.F. Kaireit, L. Behrendt, H.B. Winther, K.M. Olsson, F. Wacker, M. M. Hoeper, S. Cebotari, J. Vogel-Claussen, Comparison of dual-energy computer tomography and dynamic contrast-enhanced MRI for evaluating lung perfusion defects in chronic thromboembolic pulmonary hypertension, PLoS One 16 (2021), e0251740, https://doi.org/10.1371/journal.pone.0251740.
[36] J. Glandorf, F. Klimeš, L. Behrendt, A. Voskrebenzev, T.F. Kaireit, M. Gutberlet, F. Wacker, J. Vogel-Claussen, Perfusion quantification using voxel-wise proton density and median signal decay in PREFUL MRI, Magn. Reson. Med. 86 (2021) 1482–1493, https://doi.org/10.1002/mrm.28787.
[37] C. Schoenfeld, S. Cebotari, J. Hinrichs, J. Renne, T. Kaireit, K.M. Olsson, A. Voskrebenzev, M. Gutberlet, M.M. Hoeper, T. Welte, A. Haverich, F. Wacker, J. Vogel-Claussen, MR imaging-derived regional pulmonary parenchymal perfusion and cardiac function for monitoring patients with chronic thromboembolic pulmonary hypertension before and after pulmonary endarterectomy, Radiology 279 (2016) 925–934, https://doi.org/10.1148/radiol.2015150765.
[38] C. Schoenfeld, J.B. Hinrichs, K.M. Olsson, M.A. Kuettner, J. Renne, T. Kaireit, C. Czerner, F. Wacker, M.M. Hoeper, B.C. Meyer, J. Vogel-Claussen, Cardio-pulmonary MRI for detection of treatment response after a single BPA treatment session in CTEPH patients, Eur. Radiol. 29 (2019) 1693–1702, https://doi.org/10.1007/s00330-018-5696-4.
[39] A. Hansch, P. Kohlmann, U. Hinneburg, J. Boettcher, A. Malich, G. Wolf, H. Laue, A. Pfeil, Quantitative evaluation of MR perfusion imaging using blood pool contrast agent in subjects without pulmonary diseases and in patients with pulmonary embolism, Eur. Radiol. 22 (2012) 1748–1756, https://doi.org/10.1007/s00330-012-2428-z.
[40] T.F. Kaireit, S.A. Sorrentino, J. Renne, C. Schoenfeld, A. Voskrebenzev, M. Gutberlet, A. Schulz, P.M. Jakob, G. Hansen, F. Wacker, T. Welte, B. Tümmler, J. Vogel-Claussen, Functional lung MRI for regional monitoring of patients with cystic fibrosis, PLoS One 12 (2017), e0187483, https://doi.org/10.1371/journal.pone.0187483.
[41] A. Tomasian, M.S. Krishnam, D.G. Lohan, A.N. Moghaddam, J.P. Finn, Adult Tetralogy of Fallot: Quantitative Assessment of Pulmonary Perfusion With Time-Resolved Three Dimensional Magnetic Resonance Angiography, Invest. Radiol. 44 (2009) 31–37, https://doi.org/10.1097/RLI.0b013e31818d385b.
[42] J. Hansmann, Correlation analysis of dual-energy CT iodine maps with quantitative pulmonary perfusion MRI, World J. Radiol. 5 (2013) 202, https://doi.org/10.4329/wjr.v5.i5.202.
[43] Y. Ohno, K. Murase, T. Higashino, M. Nogami, H. Koyama, D. Takenaka, H. Kawamitu, S. Matsumoto, H. Hatabu, K. Sugimura, Assessment of bolus injection protocol with appropriate concentration for quantitative assessment of pulmonary perfusion by dynamic contrast-enhanced MR imaging, J. Magn. Reson. Imaging 25 (2007) 55–65, https://doi.org/10.1002/jmri.20790.
[44] K. Hueper, M.A. Parikh, M.R. Prince, C. Schoenfeld, C. Liu, D.A. Bluemke, S. M. Dashnaw, T.A. Goldstein, E.A. Hoffman, J.A. Lima, J. Skrok, J. Zheng, R.G. Barr, J. Vogel-Claussen, Quantitative and semiquantitative measures of regional pulmonary microvascular perfusion by magnetic resonance imaging and their relationships to global lung perfusion and lung diffusing capacity: The multiethnic study of atherosclerosis chronic obstructive pulmonary disease study, Invest. Radiol. 48 (2013) 223–230, https://doi.org/10.1097/RLI.0b013e318281057d.
[45] O. Bane, S.J. Hectors, M. Wagner, L.L. Arlinghaus, M.P. Aryal, Y. Cao, T. L. Chenevert, F. Fennessy, W. Huang, N.M. Hylton, J. Kalpathy-Cramer, K. E. Keenan, D.I. Malyarenko, R.V. Mulkern, D.C. Newitt, S.E. Russek, K.F. Stupic, A. Tudorica, L.J. Wilmes, T.E. Yankeelov, Y. Yen, M.A. Boss, B. Taouli, Accuracy, repeatability, and interplatform reproducibility of T1 quantification methods used for DCE-MRI: Results from a multicenter phantom study, Magn Reson Med. 79 (2018) 2564–2575, https://doi.org/10.1002/mrm.26903.
[46] J.K. Wiencke, K.T. Kelsey, Teen smoking, field cancerization, and a "critical period" hypothesis for lung cancer susceptibility, Environ. Health Perspect. 110 (2002) 555–558, https://doi.org/10.1289/ehp.02110555.
[47] C. Fink, S. Ley, F. Risse, M. Eichinger, J. Zaporozhan, R. Buhmann, M. Puderbach, C. Plathow, H.-U. Kauczor, Effect of inspiratory and expiratory breathhold on pulmonary perfusion assessment by pulmonary perfusion magnetic resonance imaging, Invest. Radiol. 40 (2005) 72–79, https://doi.org/10.1097/01.rli.0000149252.42679.78.
[48] L. Pstras, K. Thomaseth, J. Waniewski, I. Balzani, F. Bellavere, The Valsalva manoeuvre: physiology and clinical examples, Acta Physiol. 217 (2016) 103–119, https://doi.org/10.1111/apha.12639.
[49] N.D. Weatherley, J.A. Eaden, P.J.C. Hughes, M. Austin, L. Smith, J. Bray, H. Marshall, S. Renshaw, S.M. Bianchi, J.M. Wild, Quantification of pulmonary perfusion in idiopathic pulmonary fibrosis with first pass dynamic contrast-enhanced perfusion MRI, Thorax 76 (2021) 144–151, https://doi.org/10.1136/thoraxjnl-2019-214375.
[50] R.S. Kuzo, R.A. Pooley, J.E. Crook, M.G. Heckman, T.C. Gerber, Measurement of caval blood flow with MRI during respiratory maneuvers: Implications for vascular contrast opacification on pulmonary CT angiographic studies, Am. J. Roentgenol. 188 (2007) 839–842, https://doi.org/10.2214/AJR.06.5035.

[51] F. Molinari, C. Fink, F. Risse, S. Tuengerthal, L. Bonomo, H.-U. Kauczor, Assessment of differential pulmonary blood flow using perfusion magnetic resonance imaging, Invest. Radiol. 41 (2006) 624–630, https://doi.org/10.1097/01.rli.0000225399.65609.45.
[52] Y. Ohno, H. Hatabu, T. Higashino, D. Takenaka, H. Watanabe, Y. Nishimura, M. Yoshimura, K. Sugimura, Dynamic perfusion MRI versus perfusion scintigraphy: Prediction of postoperative lung function in patients with lung cancer, Am. J. Roentgenol. 182 (2004) 73–78, https://doi.org/10.2214/ajr.182.1.1820073.
[53] G. Bauman, O. Bieri, Matrix pencil decomposition of time-resolved proton MRI for robust and improved assessment of pulmonary ventilation and perfusion, Magn. Reson. Med. 77 (2017) 336–342, https://doi.org/10.1002/mrm.26096.
[54] Å. Kjørstad, D.M.R. Corteville, A. Fischer, T. Henzler, G. Schmid-Bindert, F. G. Zöllner, L.R. Schad, Quantitative lung perfusion evaluation using fourier decomposition perfusion MRI, Magn. Reson. Med. 72 (2014) 558–562, https://doi.org/10.1002/mrm.24930.
[55] G.M. Lu, Y. Zhao, L.J. Zhang, U.J. Schoepf, Dual-energy CT of the lung, Am. J. Roentgenol. 199 (2012) S40–S53, https://doi.org/10.2214/AJR.12.9112.
[56] M.-J. Kang, C.M. Park, C.-H. Lee, J.M. Goo, H.J. Lee, Dual-energy CT: Clinical applications in various pulmonary diseases, Radiographics 30 (2010) 685–698, https://doi.org/10.1148/rg.303095101.
[57] P. Felloni, A. Duhamel, J.-B. Faivre, J. Giordano, S. Khung, V. Deken, J. Remy, M. Remy-Jardin, Regional distribution of pulmonary blood volume with dual-energy computed tomography, Acad. Radiol. 24 (2017) 1412–1421, https://doi.org/10.1016/j.acra.2017.05.003.
[58] A. Seraphim, K.D. Knott, K. Menacho, J.B. Augusto, R. Davies, I. Pierce, G. Joy, A. N. Bhuva, H. Xue, T.A. Treibel, J.A. Cooper, S.E. Petersen, M. Fontana, A. D. Hughes, J.C. Moon, C. Manisty, P. Kellman, Prognostic value of pulmonary transit time and pulmonary blood volume estimation using myocardial perfusion CMR, J. Am. Coll. Cardiol. Img. 14 (2021) 2107–2119, https://doi.org/10.1016/j.jcmg.2021.03.029.
[59] M. Kanski, H. Arheden, D.M. Wuttge, G. Bozovic, R. Hesselstrand, M. Ugander, Pulmonary blood volume indexed to lung volume is reduced in newly diagnosed systemic sclerosis compared to normals – A prospective clinical cardiovascular magnetic resonance study addressing pulmonary vascular changes, J. Cardiovasc. Magn. Reson. 15 (2013) 86, https://doi.org/10.1186/1532-429X-15-86.
[60] M. Salehi Ravesh, G. Brix, F.B. Laun, T.A. Kuder, M. Puderbach, J. Ley-Zaporozhan, S. Ley, A. Fieselmann, M.F. Herrmann, W. Schranz, W. Semmler, F. Risse, Quantification of pulmonary microcirculation by dynamic contrast-enhanced magnetic resonance imaging: Comparison of four regularization methods, Magn. Reson. Med. 69 (2013) 188–199, https://doi.org/10.1002/mrm.24220.
[61] L.C. Bell, K. Wang, A.M. del Rio, T.M. Grist, S.B. Fain, S.K. Nagle, Comparison of models and contrast agents for improved signal and signal linearity in dynamic contrast-enhanced pulmonary magnetic resonance imaging, Invest. Radiol. 50 (2015) 174–178, https://doi.org/10.1097/RLI.0000000000000122.
[62] H. Hatabu, E. Tadamura, D.L. Levin, Q. Chen, W. Li, D. Kim, P.v. Prasad, R. R. Edelman, Quantitative Assessment of Pulmonary Perfusion With Dynamic Contrast-Enhanced MRI, Magn. Res. Med. 42 (1999) 1033–1038, https://doi.org/10.1002/(SICI)1522-2594(199912)42:6<1033::AID-MRM7>3.0.CO;2-7.
[63] S. Ley, M. Puderbach, F. Risse, J. Ley-Zaporozhan, M. Eichinger, D. Takenaka, H.-U. Kauczor, M. Bock, Impact of Oxygen Inhalation on the Pulmonary Circulation Assessment by Magnetic Resonance (MR)-Perfusion and MR-Flow Measurements, Invest. Radiol. 42 (2007) 283–290, https://doi.org/10.1097/01.rli.0000258655.58753.5d.
[64] J. Ley-Zaporozhan, F. Molinari, F. Risse, M. Puderbach, J.-P. Schenk, A. Kopp-Schneider, H.-U. Kauczor, S. Ley, Repeatability and reproducibility of quantitative whole-lung perfusion magnetic resonance imaging, J. Thorac. Imag. 26 (2011) 230–239, https://doi.org/10.1097/RTI.0b013e3181e48c36.
[65] F. Risse, W. Semmler, H.U. Kauczor, C. Fink, Dual-bolus approach to quantitative measurement of pulmonary perfusion by contrast-enhanced MRI, J. Magn. Reson. Imaging 24 (2006) 1284–1290, https://doi.org/10.1002/jmri.20747.
[66] S. Veldhoen, M. Oechsner, A. Fischer, A.M. Weng, A.S. Kunz, T.A. Bley, H. Köstler, C.O. Ritter, Dynamic contrast-enhanced magnetic resonance imaging for quantitative lung perfusion imaging using the dual-bolus approach: Comparison of 3 contrast agents and recommendation of feasible doses, Invest. Radiol. 51 (2016) 186–193, https://doi.org/10.1097/RLI.0000000000000224.